Role of infection on the stability of a predator–prey system with several response functions—A comparative study

N. Bairagi[a], P.K. Roy[b,1], J. Chattopadhyay[c,*]

[a]Centre for Mathematical Biology and Ecology, Department of Mathematics, Jadavpur University, Kolkata-700032, India
[b]Department of Mathematics, Barasat Government College, Kolkata-700124, India
[c]Agricultural and Ecological Research Unit, Indian Statistical Institute, 203, B.T. Road, Kolkata-700108, India

Abstract

In this paper, we have proposed and analyzed a mathematical model of an infected predator–prey system with different predators' functional response. The existence and uniqueness of solutions are established and solutions are shown to be uniformly bounded for all nonnegative initial values. Our overall mathematical and biological studies reveal that if the prey population is infected by a lethal disease, coexistence of all three species (i.e. host, parasite and predator) for any of three functional responses is never possible but different interesting dynamical behaviors are possible by varying two key parameters viz. the rate of infection and the attack rate on susceptible prey. Interplay between these two factors yields a diverse array of biologically relevant behavior, including switching of stability, extinction and oscillations.

Keywords: Susceptible population; Infected population; Local stability; Global stability; Linear mass action; Holling type II and III functional response

1. Introduction

Ecology and Epidemiology are major fields of study in their own right but there are some common features between these systems. The effect of disease in ecological system is an important issue from mathematical and ecological point of view. Researchers are paying more and more interest to merge these two important areas of research (Hadeler and Freedman, 1989; Freedman, 1990; Beltrami and Carroll, 1994; Beretta and Kuang, 1998; Venturino, 1995; Chattopadhyay and Arino, 1999; Chattopadhyay and Bairagi, 2001; Xiao and Chen, 2001; Chattopadhyay and Pal, 2002; Venturino, 2002; Hethcote et al., 2004). Eco-epidemiology is a new branch in mathematical biology which considers both the ecological and epidemiological issues simultaneously. Successful invasion of a parasite into a host population and resulting host–parasite dynamics can depend crucially on other members of a host's community such as predators (Hall et al., 2005). On the other hand, predation intensity can dramatically shape community structure and ecosystem properties (Sih et al., 1985). Predation becomes particularly interesting in host–parasite systems because predation itself can strongly alter population dynamics of hosts and parasites (Ives and Murray, 1997; Hudson et al., 1998; Packer et al., 2003; Dwyer et al., 2004). Predators may even prevent successful invasion of parasites into host population. Also, in most theoretical studies of host–parasite–predation interactions, predator behavior is simplified and isolated from an ecosystem (Packer et al., 2003). Another important point is the choice of functional response which is defined as the amount of prey catch per predator per unit of time. The functional response encapsulates attributes of both predator and prey biology. It is affected by prey escape ability, structure of the prey habitat and by the time predator require to subdue and consume prey before beginning to hunt again i.e. predator's hunting ability (Alstad, 2001; Anderson, 2001). Here, we propose

a host–parasite–predator model and study how the dynamics of the system depend on the infection rate, attack rate and also on the nature of the predators' functional response.

Venturino (1995) studied an *SI* or *SIS* models with disease spread among the prey when there is logistic growth on the predator population as well as on the prey and the predators eat infected prey only. Chattopadhyay and Arino (1999) proposed a three species eco-epidemiological model, namely, sound prey (susceptible), infected prey (infective), and their predator and found the conditions for local stability, extinction and Hopf-bifurcation. Hethcote et al. (2004) modified a predator–prey model with logistic growth in the prey with an SIS disease in the prey population, They assumed that infected prey are more vulnerable to predation to susceptible prey, and consumed prey (both susceptible and infected) contribute positive growth to the predator population. Deficiencies in these models are that predators eat infected prey only and consumption of infected prey contribute positive growth to the predator population. But in general cases, predators not only prey infected preys but susceptible preys also. Again, it is frequently observed in nature that consumption of infected prey becomes fatal to the predator population. In such situations, one must keep in mind that consumption of infected prey will contribute negative growth in the predator population.

The most commonly used functional response in a predator–prey interaction is linear. If a predator's handling time for prey is zero, then predation term follow a linear mass-action functional response, $h(N)$ and has the form $h(N) = \alpha N$, α being the attack rate and N being the prey density. It implies that there will be no upper limit to the prey consumption rate of the predator, a prediction that is too simple to reflect nature (but see Korpimaki and Norrdahl, 1991). Although, the mass-action functional response is mathematically convenient, predators often become satiated in nature. Holling type II and III functional responses (Holling, 1959) have this satiated property when prey density is high. The type II response, is an asymptotic curve that decelerates constantly as prey number increase due to the time it takes the predator to manipulates its prey (i.e. the handling time). The asymptote reflects the maximum attack rate. The mathematical representation of most commonly used type II form is $\frac{\alpha N}{a+N}$, a being the half-saturation constant. The type III response function is sigmoid, rising slowly when prey are rare, accelerating when they become more abundant, and finally reaching a saturated upper limit. The mathematical representation of a type III functional response is $\frac{\alpha N^2}{a^2+N^2}$. Holling (1959), in his classical paper, suggested that the type II responses are characteristic of predators which have no learning ability or when given only one type of prey for which to search, whereas type III responses are characteristic of vertebrate predators where switching and learning are more common (Ricklefs and Miller, 2000).

Many biological factors ought to alter the form of predator's functional response and thereby alter the dynamics of the predator and prey populations. Since functional response encapsulates attributes of both predator and prey biology, so handling time, search efficiency, encounter rate, prey escape ability, etc. should alter, in general, the functional response (Alstad, 2001; Ricklefs and Miller, 2000). Therefore, predators' functional response may be different when a particular predator preys different prey having different escape ability. Again, if a particular prey be predated by different predators, the functional response may be different due to their different hunting ability. Furthermore, structure of the prey habitat is also responsible to alter the functional response. The type II response function describes a situation in which the number of prey consumed per predator initially rises quickly as the density of prey increases and then level off. Type III functional response also levels off at some prey density. However, the type III functional response curve behaves differently than the type II curve when the prey density is low. A heterogeneous habitat may afford a limited number of safe hiding places, which protect a larger portion of the prey at lower densities (Ricklefs and Miller, 2000). This heterogeneous habitat reduce predation rates by decreasing encounter rates between predator and prey (Anderson, 1984; Sih, 1987). Thus, a predator which follows type II response function in homogeneous habitat may follow type III in a heterogeneous medium. Anderson (2001) observed experimentally in a predator–prey (kelp bass-kelp parch) interaction for none and medium amounts of habitat structure, the type II functional response had a better fit than linear models. However, for the highest amount of habitat structure a type III functional response had a better fit. His experiment provides evidence that response function of a particular predator to a particular prey may be different depending on the structural complexity of the prey habitat. Therefore, a model could be more realistic from ecological point of view and interesting from mathematical point of view if one considers different predators' functional response and compares the dynamic effects of these functional responses. Let us now think of an ideal situation where these ecological and epidemiological characteristics can be fitted. Consider a large aquatic region having different fish species (prey) with different sizes having different escape abilities. Assume that different fish-eating birds (predator) having different hunting abilities prey on same/different fish species with different sizes. It is also quite natural that in a large aquatic body there exists habitat complexity which causes the asymmetric predator–prey interaction and thus providing prey refuges for different species to different degree. This idealized predator–prey interaction ought to be modelled with different predator's response function. Now if the prey population is infected by some parasites, infection may spread into the predator population through predator–prey interaction and it may cause death of both prey and predator populations if the infection be lethal.

In this paper, we propose and analyze a mathematical model which has the aforesaid eco-epidemiological

properties. The aim is to study and compare the dynamics of the proposed eco-epidemiological model to explore the crucial system parameters and their ranges in order to obtain different theoretical behaviors predicted from the interactions between susceptible prey, infected prey and their predators.

The organization of the paper is as follows: Section 2 deals with the mathematical model; existence, uniqueness and boundedness of the solutions are presented in Section 3. Stability analysis are presented in Sections 4, 5 and 6 for linear mass-action law, Holling type II and III response functions, respectively. Numerical simulations and discussion are presented in Section 7. Moreover, a real life problem on grouse population has been considered as a case study in Section 7.

2. Development of the model

SI epidemic model: A typical *SI* model with an open system of variable size can be written as follows:

$$\frac{dS}{dt} = S\phi(S) - \psi(S,I),$$
$$\frac{dI}{dt} = \psi(S,I) - \mu I, \tag{2.1}$$

where S and I are the densities of susceptible and infected population respectively, $\phi(S)$ is the intrinsic growth rate of the susceptible population, $\psi(S,I)$ is incidence of the disease i.e. the rate at which infections occur and μ is the sum of the death rate due to disease and the natural death rate. It is assumed that all susceptible population are equally susceptible and all infected population are equally infectious. It is also assumed that the disease is transmitted by contact between an infected and susceptible population following the law of mass action, so that $\psi(S,I) = \lambda SI$, where λ is known as (pair wise) infectious contact rate i.e. the rate of infection per susceptible and per infective.

Predator–prey model: A general predator–prey model in its classical form is represented by

$$\frac{dN}{dt} = Nf(N) - Ph(N),$$
$$\frac{dP}{dt} = \theta Ph(N) - \delta P, \tag{2.2}$$

where N and P are, respectively, the densities of prey and predator population. $f(N)$ is the per capita growth rate of prey in the absence of predation and δ is the food independent predator mortality, which is assumed to be constant. Here $h(N)$ is the functional response and the term $\theta h(N)$ is known as the numerical response of the predator, θ being the conversion efficiency. We assume that the function f grows logistically with intrinsic growth rate r and carrying capacity K so that $f(N) = r(1 - \frac{N}{K})$.

Now we are in a position to formulate the basic eco-epidemiological model combining the *SI* epidemic model (2.1) and the predator–prey model (2.2).

Eco-epidemiological model: The following assumptions are made in formulating the basic eco-epidemiological model:

(A1) In the absence of infection and predation, the prey population grows logistically.

(A2) In the presence of infection, the prey population are divided into two disjoint classes, namely, susceptible population, S, and infected population, I.

(A3) It is assumed that only susceptible population, S, are capable of reproducing with logistic law and the infective population I, dies before having the capability of reproducing. However, the infective population, I, still contributes with S to population growth towards the carrying capacity.

(A4) The mode of disease transmission follows the simple law of mass action. The disease is spread among the prey population only and the disease is not genetically inherited. The infected population do not recover or become immune.

(A5) It is assumed that predator cannot distinguish the infected and healthy prey, they consume both the susceptible and infected preys at the rates $h(S)$ and $g(I)$, respectively. Feeding on infected prey enhances the death rate of predator and is considered to contribute negative growth where as feeding on susceptible prey enhances the growth rate and is considered to contribute positive growth.

(A6) Since infected preys are weakened and become easier to catch (Moore, 2002; Murray et al., 1997; Hudson et al., 1992a,b), we assume for simplicity that predators' handling time for infected prey is zero. Therefore, the predation term for infected prey follows a linear mass-action functional response (Hall et al., 2005) i.e. $g(I) = \beta I$, β being the attack rate on infected prey. However, as mentioned in the introduction, it would be theoretically interesting to investigate the effects of different response functions for susceptible prey. In particular, we assume the predator response function, $h(S)$, for susceptible prey as linear, Holling type-II and III.

Based on the above assumptions we have the following equations as our eco-epidemiological model:

$$\frac{dS}{dt} = rS\left(1 - \frac{S+I}{K}\right) - \lambda IS - h(S)P,$$
$$\frac{dI}{dt} = \lambda IS - \beta IP - \mu I,$$
$$\frac{dP}{dt} = -\theta\beta IP - \delta P + \theta h(S)P. \tag{2.3}$$

System (2.3) has to be analyzed with the initial condition

$$S(0) > 0, \quad I(0) > 0, \quad P(0) > 0,$$

with three different forms of $h(S)$ viz. linear, Holling type-II and III. Model conceptual schematic diagram is presented in Fig. 1.

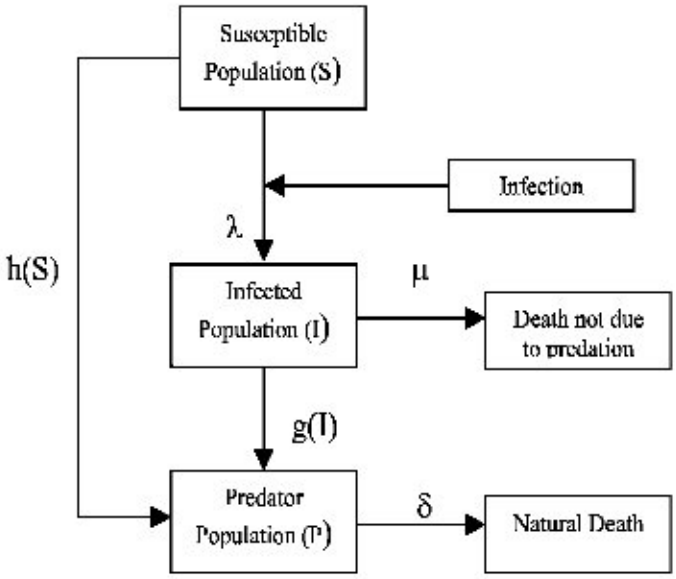

Fig. 1. Schematic diagram of the eco-epidemiological (2.3).

Chattopadhyay et al. (2003) studied this eco-epidemiological problem, where they assumed predators' response function as type II only. Keeping in mind the importance of such problems it is essential to study and compare the results rigorously with different functional response.

Empirical and experimental evidences: Salton Sea in California has come in the limelight for its massive fish and fish-eating bird mortality event due to bloom of botulism bacteria. Each year millions of birds are paralyzed or die after consuming infected fish. It is well known that fish species are infected by a vibrio class of bacteria. As the fish struggle in their death they tend to rise to the surface of the sea and become more vulnerable as well as attractive to different fish-eating birds. Predatory birds get disease only from eating infected prey; also the disease does not spread from one predator to another. Infected fish dies off within a few days, thus removing the chances of reproduction by the infected fish but still they contribute to the carrying capacity. Vibrio is passed from one infected fish to another susceptible fish; the more fish that are in the sea, the more chance that a large number of them will be infected by the disease. This causes terrible bird mortality events at the Salton Sea (for details see Gonzalez et al., 1998; Steve Horvitz http://www.sci.sdsu.edu/salton/Salton%20Sea%20Description.html). Salton Sea is over crowded with different fish species and so we can assume that the reproduction process is continuous and thus meeting several assumptions of continuous time models. Thus the eco-epidemiological situations of the Salton Sea are meeting most of the assumptions made for the model formulation.

Hudson and his colleagues made a series of field studies and experiments on an eco-epidemiological problem of upland estates in England and Scotland. Intensive studies on red grouse (prey) and their predator (mainly fox) reveals that prey vulnerability increases with the parasite burden in prey (Hudson et al., 1992a,b). Different experiments and observations confirm that predators capture a disproportionately high number of grouse infected with parasites (Hudson et al., 1992a,b). Population studies show that the red grouse exhibit cyclic changes with average cycle lengths 4 to 5 years in population density in some estates (Potts et al., 1984), although it does not occur in all estates (Hudson and Dobson, 1990). Numerical study of this eco-epidemiological system will be performed in Section 7 as a case study.

3. Existence, uniqueness and boundedness

The right-hand side of Eq. (2.3) are smooth functions of the variables S, I, P and parameters, as long as these quantities are nonnegative, so local existence, uniqueness and continuation properties hold in the positive octant for some time interval $(0, t_f)$. In the next theorem we show that the linear combination of susceptible prey, infected prey and predator population is less than a finite quantity or in other words, the solution of system (2.3) is bounded.

Theorem 3.1. *The solution* $y(t)$ *of* (2.3), *where* $y = (S, I, P)$, *is uniformly bounded for* $y_0 \in R^3_{0,+}$.

Proof. We define a function $W(t) : R_{0,+} \to R_{0,+}$ by

$$W(t) = S + I + \frac{1}{\theta}P.$$

Observe that W is well defined and differentiable on some maximal interval $(0, t_f)$.

Now, for any $\eta > 0$, we have

$$\frac{dW(t)}{dt} + \eta W(t) \leqslant \frac{K(r+\eta)^2}{4r} - (\mu - \eta)I - (\delta - \eta)\frac{P}{\theta}.$$

If we assume that, $0 < \eta < \min(\mu, \delta)$, then there exists $B > 0$ such that

$$\frac{dW(t)}{dt} + \eta W(t) \leqslant B \quad \text{for each } t \in (0, t_f).$$

Let $G(t, y) = B - \eta y$, which satisfies Lipschtiz condition everywhere. Clearly,

$$\frac{dW(t)}{dt} \leqslant B - \eta W(t) = G(t, W(t)) \quad \text{for all } t \in (0, t_f).$$

Let

$$\frac{dx}{dt} = G(t, x) = B - \eta x \quad \text{and} \quad x(0) = W(0) = W_0.$$

This ordinary differential equation has the solution

$$x(t) = \frac{B}{\eta}(1 - e^{-\eta t}) + W_0 e^{-\eta t}.$$

It is clear that $x(t)$ is bounded on $(0, t_f)$. By comparison theorem (Birkhoff and Rota, 1989)

$$W(t) \leqslant x(t) = \frac{B}{\eta}(1 - e^{-\eta t}) + W_0 e^{-\eta t} \quad \forall t \in (0, t_f).$$

Now suppose $t_f < \infty$. Then $W(t_f) \leqslant x(t_f) < \infty$, but then the solution exists uniquely for some interval $(0, t_f)$ by the Picard–Lindelof Theorem. This contradicts the supposition

that $t_f<\infty$. Therefore, $W(t)$ must be bounded for all nonnegative t and thus $y(t)$ is uniformly bounded on $R_{0,+}$.

In the next section we first consider the commonly used linear mass-action functional response.

4. Linear mass-action functional response

For type I response function, system (2.3) takes the following form:

$$\frac{dS}{dt}=rS\left(1-\frac{S+I}{K}\right)-\lambda SI-\alpha SP,$$
$$\frac{dI}{dt}=\lambda SI-\beta IP-\mu I,$$
$$\frac{dP}{dt}=-\theta\beta IP-\delta P+\theta\alpha SP. \tag{4.1}$$

Applying the transformations $s=\frac{S}{K}, i=\frac{I}{K}, p=\frac{P}{K}, \tau=\lambda Kt$ we have the following dimensionless form of the model equation (4.1). Henceforth, we will replace τ by t for notational convenience.

$$\frac{ds}{dt}=bs(1-(s+i))-si-m_1sp,$$
$$\frac{di}{dt}=si-dip-ei,$$
$$\frac{dp}{dt}=-\theta dip-gp+\theta m_1sp, \tag{4.2}$$

where $b=\frac{r}{\lambda K}, m_1=\frac{\alpha}{\lambda}, d=\frac{\beta}{\lambda}, e=\frac{\mu}{\lambda K}$ and $g=\frac{\delta}{\lambda K}$.

4.1. Equilibria and local stability

System (4.2) has the following equilibria: $E_0^I=(0,0,0)$, $E_1^I=(1,0,0)$, $E_2^I=(e,\frac{b(1-e)}{b+1},0)$, $E_3^I=(\frac{g}{\theta m_1},0,\frac{b(\theta m_1-g)}{\theta m_1^2})$ and $E_*^I=(s^*,i^*,p^*)$, where,

$$s^*=\frac{bd\theta+m_1e\theta+bg+g}{\theta(bd+bm_1+2m_1)},$$
$$i^*=\frac{m_1\theta s^*-g}{d\theta},$$
$$p^*=\frac{s^*-e}{d},$$
$$\text{and}\quad s^*+i^*\leqslant 1. \tag{4.3}$$

The last condition of (4.3) is due to the fact that $s(t)+i(t)\leqslant 1, \forall t>0$.

The equilibria E_0^I and E_1^I exist for all parameter values. E_2^I exists if $e<1$. E_3^I exists if $m_1>\frac{g}{\theta}$. The interior equilibrium E_*^I exists if

$$e<1,\quad m_1>\frac{g}{\theta}\quad\text{and}\quad\left(e,\frac{g}{m_1\theta}\right)<s^*<\frac{g+d\theta}{\theta(m_1+d)}.$$

Observe that E_2^I arises from E_1^I for $e=1$ and persists for all $e<1$, whereas E_3^I arises from E_1^I for $m_1=\frac{g}{\theta}$ and persists for all $m_1>\frac{g}{\theta}$. If $e=1$ and $m_1=\frac{g}{\theta}$, then E_2^I and E_3^I will approach E_1^I which biologically means eventually eradication of infected population and predator population.

The variational matrix about any arbitrary equilibrium $E(s,i,p)$ is given by

$$\begin{pmatrix} b-2bs-bi-i-m_1p & -bs-s & -m_1s \\ i & s-dp-e & -di \\ m_1\theta p & -d\theta p & -d\theta i-g+m_1\theta s \end{pmatrix}.$$

Now we state and prove the following theorems:

Theorem 4.1. *System (4.2) is unstable around E_0^I for all parametric values. (The proof is obvious.)*

Theorem 4.2. *System (4.2) is locally asymptotically stable around E_1^I if $e>1$ and $m_1<\frac{g}{\theta}$. In fact, then the system is globally asymptotically stable.*

Proof. The characteristic roots corresponding to E_1^I are given by

$$\xi_{1,1}^I=-b,\quad \xi_{2,1}^I=1-e\quad\text{and}\quad \xi_{3,1}^I=m_1\theta-g.$$

Thus E_1^I is stable if $e>1$ and $m_1<\frac{g}{\theta}$. In fact, in this case E_1^I becomes globally stable, as stability conditions of E_1^I eliminate the existence of E_2^I, E_3^I, E_*^I. In this case, all solutions initiating on the ip-plane approach E_0^I and all other solutions with initial values $R_{0,+}^3\backslash\{ip\text{-plane}\}$ will approach E_1^I as we have $\frac{di}{dt}<0$ and $\frac{dp}{dt}<0$ whenever conditions of Theorem 4.2 hold. Hence the theorem. □

Theorem 4.3. *System (4.2) is locally asymptotically stable around E_2^I if $e<1$ and $m_1<\frac{1}{e\theta}[g+\frac{bd\theta(1-e)}{b+1}]$. In fact, E_2^I is globally asymptotically stable.*

Proof. Observe that when $\xi_{2,1}^I>0$ (i.e. $e<1$) and $\xi_{3,1}^I<0$ (i.e. $m_1<\frac{g}{\theta}$), then system (4.2) admits E_0^I, E_1^I and E_2^I as its equilibrium points. Clearly, E_0^I is always unstable and E_1^I is unstable with sp-plane and i-axis as its stable and unstable manifolds.

Studying the variational matrix corresponding to E_2^I one can observe that the eigenvalue in the p-direction is given by $\xi_{3,2}^I=m_1e\theta-g-\frac{bd\theta(1-e)}{b+1}$ and it is negative if $m_1<\frac{1}{e\theta}[g+\frac{bd\theta(1-e)}{b+1}]$. Other two eigenvalues are the roots of the quadratic equation

$$\xi^2+be\xi+be(1-e)=0.$$

Obviously, both roots of this quadratic equation are real negative or complex conjugate with negative real parts. Hence E_2^I is locally asymptotically stable if $m_1<\frac{1}{e\theta}[g+\frac{bd\theta(1-e)}{b+1}]$.

Note that when E_1^I becomes unstable with i-axis its unstable manifold and sp-plane its stable manifold, then still $\xi_{3,2}^I<0$ and E_2^I becomes locally asymptotically stable. Since $\xi_{3,1}^I<0$ (i.e. $m_1<\frac{g}{\theta}$) implies $\frac{dp}{dt}<0$, from the third equation of (4.2), hence all solutions initiating in the interior of the positive octant will approach si-plane. In fact, E_2^I will be globally stable in this case if the conditions of Theorem 4.3 are satisfied. □

If $\xi^I_{2,1}<0$ (i.e. $e>1$) and $\xi^I_{3,1}>0$ (i.e. $m_1>\frac{g}{\theta}$) then system (4.2) admits three equilibria viz. E^I_0, E^I_1, E^I_3. In this case E^I_1 is saddle with *si*-plane its stable manifold and *p*-axis as unstable manifold, whereas E^I_0 is always unstable saddle. Thus, only solutions with initial values in the *si*-plane approaches E^I_1 and those with initial values in the interior of the *sp*-plane will either approach E^I_3 or a stable limit cycles surrounding E^I_3 if it is stable or unstable in the *sp*-plane. In the next theorem we will observe this phenomenon.

Theorem 4.4. *The sufficient conditions for asymptotic stability of E^I_3 is $m_1>\frac{g}{e\theta}$ or $m_1>\frac{g}{\theta}$ according as $e<1$ or $e>1$.*

Proof. The characteristic equation corresponding to E^I_3 is given by

$$(-\xi-dp-e+s)(\xi^2+b\xi+m_1^2\theta sp)=0.$$

The eigenvalue in the *i*-direction is $\xi^I_{2,3}=s-dp-e=\frac{g}{m_1\theta}-\frac{bd(m_1\theta-g)}{m_1^2\theta}-e$. The sufficient condition for $\xi^I_{2,3}$ to be negative is $m_1>\frac{g}{e\theta}$. The other eigenvalues $\xi^I_{1,3}$ and $\xi^I_{3,3}$ are the roots of the quadratic equation $\xi^2+b\xi+m_1^2\theta sp=0$. The roots of this equation are either real negative or complex conjugate with negative real parts. Also, the existence condition of E^I_3 is $m_1>\frac{g}{\theta}$. Hence the sufficient condition for the stability of E^I_3 is $m_1>\max(\frac{g}{e\theta},\frac{g}{\theta})$. Note that $\max(\frac{g}{e\theta},\frac{g}{\theta})=\frac{g}{e\theta}$ or $\frac{g}{\theta}$ according as $e<1$ or $e>1$. Since $\xi^I_{2,1}<0$ (i.e. $e>1$), we have $\frac{di}{dt}<0$. Hence all solutions initiating in the interior of the positive octant will be drawn towards the *sp*-plane and eventually approach E^I_3. Hence the theorem. □

Observation 4.1. In this case, *sp*-plane is always stable manifold of E^I_3 which restrict *sp*-plane from having a limit cycles in the *sp*-plane. If *sp*-plane would have been an unstable manifold of E^I_3 with $\xi^I_{3,2}<0$, then there would be a stable limit cycles surrounding E^I_3. We will observe this phenomenon in Theorem 5.4 in case of Holling type II response function.

Theorem 4.5. *System* (4.2) *is always unstable around E^I_* for all parametric values.*

Proof. Observe that from first two equations of system (4.2), we always have

$$\frac{d(s+i)}{dt}=bs(1-(s+i))-m_1sp-dip-ei<b(s+i)(1-(s+i)).$$

Hence from Lakshmikantham and Leela (1969), we have $\lim_{t\to\infty}\{s(t)+i(t)\}<1$. Thus we have $s^*+i^*<1$ and the last condition of (4.3) is always satisfied. It is also true for type II and type III response functions also.

The variational matrix corresponding to E^I_* is

$$V^*=\begin{pmatrix} m^I_{11} & m^I_{12} & m^I_{13}\\ m^I_{21} & m^I_{22} & m^I_{23}\\ m^I_{31} & m^I_{32} & m^I_{33}\end{pmatrix},$$

where

$$m^I_{11}=-bs^*\ (<0),\quad m^I_{12}=-(b+1)s^*\ (<0),$$

$$m^I_{13}=-m_1s^*\ (<0),$$

$$m^I_{21}=i^*\ (>0),\quad m^I_{23}=-di^*\ (<0),\quad m^I_{31}=m_1\theta p^*\ (>0),$$

$$m^I_{32}=-\theta dp^*\ (<0),\quad m^I_{22}=m^I_{33}=0.$$

The characteristic equation corresponding to this variational matrix can be put in the form

$$\xi^3+A_1\xi^2+A_2\xi+A_3=0, \tag{4.4}$$

where

$$A_1=m^I_{11},$$

$$A_2=-(m^I_{23}m^I_{32}+m^I_{31}m^I_{13}+m^I_{12}m^I_{21}),$$

$$A_3=m^I_{11}m^I_{23}m^I_{32}-m^I_{12}m^I_{31}m^I_{23}-m^I_{13}m^I_{21}m^I_{32}.$$

From Routh–Hurwitz criterion, E^I_* is locally asymptotically stable if and only if

$$A_1>0,\quad A_3>0\quad\text{and}\quad A_1A_2-A_3>0.$$

From the signs of those defined, $m^I_{ij}, i,j=1,2,3$, it is easy to verify that $A_1>0$ but $A_3<0$ for all parametric values. Thus system (4.2) is always unstable around E^I_*. This completes the theorem. □

When $\xi^I_{2,1}<0$ (i.e. $e>1$) and $\xi^I_{3,1}>0$ (i.e. $m_1>\frac{g}{\theta}$), then system (4.2) admits all the five equilibria E^I_0, E^I_1, E^I_2, E^I_3 and E^I_*. Here E^I_0, E^I_1 are saddle and E^I_* is also unstable. Hence all solutions initiating in the interior of the positive octant will drawn either towards the *si*-plane and eventually approach E^I_2 or towards the *sp*-plane and eventually approach E^I_3 (or approach a limit cycle surrounding E^I_3 in case of Holling type II) depending on whether the initial value of the system is contained in the invariant set which contain the equilibrium point E^I_2 or E^I_3, respectively.

In the next section we study the saturated Holling type II functional response.

5. Holling type II functional response

For type II response function, system (2.3) takes the following form:

$$\frac{dS}{dt}=rS\left(1-\frac{S+I}{K}\right)-\lambda SI-\frac{\alpha SP}{a+S},$$
$$\frac{dI}{dt}=\lambda SI-\beta IP-\mu I,$$
$$\frac{dP}{dt}=-\theta\beta IP-\delta P+\frac{\theta\alpha SP}{a+S}. \tag{5.1}$$

Applying the same transformations as before we have the following dimensionless form of the model equation (5.1).

$$\frac{ds}{dt} = bs(1-(s+i)) - si - \frac{m_2 sp}{1+ls},$$
$$\frac{di}{dt} = si - dip - ei,$$
$$\frac{dp}{dt} = -\theta dip - gp + \frac{\theta m_2 sp}{1+ls}, \tag{5.2}$$

where $m_2 = \frac{a}{\lambda\alpha}$ and $l = \frac{K}{a}$. Note that l, the ratio of the carrying capacity to the half-saturation constant, will be assumed to be greater than unity in the future study.

5.1. Equilibria and local stability

System (5.2) has the following equilibria: $E_0^{II} = (0,0,0)$, $E_1^{II} = (1,0,0)$, $E_2^{II} = (e, \frac{b(1-e)}{b+1}, 0)$, $E_3^{II} = (\frac{g}{\theta m_2 - g l}, 0, \frac{b\theta(\theta m_2 - gl - g)}{(\theta m_2 - gl)^2})$ and $E_*^{II} = (s^*, i^*, p^*)$, where

$$i^* = \frac{1}{d\theta}\left[\frac{m_2\theta s^*}{1+ls^*} - g\right],$$

$$p^* = \frac{s^* - e}{d}.$$

Note that $p^* > 0$ as $s^* > e$, otherwise $i \to 0$ from the second equation of (5.2) and $i^* > 0$ as $\frac{m_2\theta s^*}{1+ls^*} > g$, otherwise $p \to 0$ from the third equation of (5.2). s^* is the positive root of the equation

$$bdl\theta s^{*2} - s^*[bd\theta(l-1) + bgl + gl - m_2\theta(b+2)] - (m_2 e\theta + bg + g + bd\theta) = 0$$

and must satisfy the inequality $s^* + i^* \leqslant 1$. The sufficient condition for existence of a unique positive s^* is $m_2 < \frac{gl(b+1)+bd\theta(l-1)}{\theta(b+2)}$. Thus, the system has a unique positive interior equilibrium (s^*, i^*, p^*) if

$$\frac{g(l+1)}{\theta} < m_2 < \frac{gl(b+1)+bd\theta(l-1)}{\theta(b+2)} \quad \text{and}$$
$$s^* > \max\left[e, \frac{g}{m_2\theta - gl}\right], \quad e<1.$$

The equilibria E_0^{II} and E_1^{II} exist for all parameter values. E_2^{II} exists if $e<1$ and E_3^{II} exists if $m_2 > \frac{g(l+1)}{\theta}$. Observe that E_2^{II} arises from E_1^{II} for $e=1$ and persists for all $e<1$, whereas E_3^{II} arises from E_1^{II} for $m_2 = \frac{g(l+1)}{\theta}$ and persists for all $m_2 > \frac{g(l+1)}{\theta}$. Also observe that the existence of E_*^{II} implies the existence of the equilibria E_2^{II} and E_3^{II}.

Variational matrix studies around each equilibrium point, as in the previous section, lead to the following theorem.

Theorem 5.1. *System (5.2) is*

(i) *unstable around E_0^{II} for all parametric values,*
(ii) *globally asymptotically stable around E_1^{II} if $e>1$ and $m_2 < \frac{g(1+l)}{\theta}$,*
(iii) *globally asymptotically stable around E_2^{II} if $e<1$ and $m_2 < \frac{1+le}{e\theta}[g + \frac{bd\theta(1-e)}{b+1}]$,*
(iv)
  (a) *asymptotically stable around E_3^{II} if $\frac{g(1+el)}{e\theta} < m_2 < \frac{gl(1+l)}{\theta(l-1)}$ with $\frac{l-1}{2l} < e < 1$ or $\frac{g(1+l)}{\theta} < m_2 < \frac{gl(1+l)}{\theta(l-1)}$ with $e>1$ and*
  (b) *possesses a stable limit cycles in the sp-plane when $m_2 > \frac{gl(1+l)}{\theta(l-1)}$ with $e > \frac{l-1}{2l}$,*
(v) *unstable around E_*^{II} for all parametric values.*

Now we are in a position to consider the saturated functional response type III.

6. Holling type III functional response

For type III response function, system (2.3) takes the following form:

$$\frac{dS}{dt} = rS\left(1 - \frac{S+I}{K}\right) - \lambda SI - \frac{\alpha S^2 P}{a^2 + S^2},$$
$$\frac{dI}{dt} = \lambda SI - \beta IP - \mu I,$$
$$\frac{dP}{dt} = -\theta\beta IP - \delta P + \frac{\theta\alpha S^2 P}{a^2 + S^2}. \tag{6.1}$$

Applying the same transformations we have the following dimensionless form of the model equation (6.1).

$$\frac{ds}{dt} = bs(1-(s+i)) - si - \frac{m_3 s^2 p}{1+l^2 s^2},$$
$$\frac{di}{dt} = si - dip - ei,$$
$$\frac{dp}{dt} = -\theta dip - gp + \frac{\theta m_3 s^2 p}{1+l^2 s^2}, \tag{6.2}$$

where $m_3 = \frac{K\alpha}{\lambda a^2}$.

6.1. Equilibria and local stability

System (6.2) has the following equilibria: $E_0^{III} = (0,0,0)$, $E_1^{III} = (1,0,0)$, $E_2^{III} = (e, \frac{b(1-e)}{b+1}, 0)$, $E_3^{III} = (A, 0, \frac{b\theta A(1-A)}{g})$, where $A = \sqrt{(\frac{g}{m_3\theta - gl^2})}$ and $E_*^{III} = (s^*, i^*, p^*)$, where,

$$i^* = \frac{1}{d\theta}\left[\frac{m_3\theta s^{*2}}{1+l^2 s^{*2}} - g\right],$$

$$p^* = \frac{s^* - e}{d}.$$

Note that $p^* > 0$ as $s^* > e$, otherwise $i \to 0$ from the second equation of (6.2) and $i^* > 0$ as $\frac{m_3\theta s^{*2}}{1+l^2 s^{*2}} > g$, otherwise $p \to 0$ from the third equation of (6.2). s^* is determined from the cubic equation

$$bdl^2\theta s^{*3} + [(b+2)\theta m_3 - (bd\theta + gb + g)l^2]s^{*2} + (bd\theta - em_3\theta)s^* - (bd\theta + gb + g) = 0$$

and must satisfy the inequality $s^* + i^* \leqslant 1$.

This cubic equation has a unique positive root if coefficients of s^{*2} and s^* are both positive. For this we must have $\frac{[g(b+1)+bd\theta]l^2}{\theta(b+2)} < m_3 < \frac{bd}{e}$. Thus, system (6.2) has a unique positive interior equilibrium (s^*, i^*, p^*) if

$$\max\left[\frac{g(1+l^2)}{\theta}, \frac{[g(b+1)+bd\theta]l^2}{\theta(b+2)}\right] < m_3 < \frac{bd}{e}$$

and

$$s^* > \max\left[e, \sqrt{\left(\frac{g}{m_3\theta - gl^2}\right)}\right], \quad e<1.$$

The equilibria E_0^{III} and E_1^{III} exist for all parameter values. E_2^{III} exists if $e<1$ and E_3^{III} exists if $m_3 > \frac{g(l^2+1)}{\theta}$.

Now we state the following theorem:

Theorem 6.1. *System* (6.2) *is*

(i) *unstable around* E_0^{III} *for all parametric values,*
(ii) *globally asymptotically stable around* E_1^{III} *if* $e>1$ *and* $m_3 < \frac{g(1+l^2)}{\theta}$,
(iii) *globally asymptotically stable around* E_2^{III} *if* $e<1$ *and* $m_3 < \frac{1+l^2e^2}{e^2\theta}[g + \frac{bd\theta(1-e)}{b+1}]$,
(iv) *asymptotically stable around* E_3^{III} *if* $m_3 > \frac{2gl^2}{\theta}$ *or* $m_3 > (\frac{gl^2}{\theta} + \frac{g}{e^2\theta})$ *according as* $l > \frac{1}{e}$ *or* $l < \frac{1}{e}$,
(v) *unstable around* E_*^{III} *for all parametric values.*

Proof. One can easily prove (i)–(iii) and (v) by studying the variational matrix, so we give the proof of (iv) only. The characteristic equation corresponding to the equilibrium E_3^{III} is given by (4.4) where

$$A_1 = -(m_{11}^{III} + m_{22}^{III}),$$

$$A_2 = -m_{13}^{III}m_{31}^{III} + m_{11}^{III}m_{22}^{III},$$

$$A_3 = m_{13}^{III}m_{31}^{III}m_{22}^{III},$$

with $m_{11}^{III} = b(1-2A) - \frac{2b(1-A)}{1+l^2A^2}, m_{12}^{III} = -A(1+b)$ (<0), $m_{13}^{III} = -\frac{g}{\theta}$ $(<0), m_{22}^{III} = A - \frac{bd\theta A(1-A)}{g} - e, m_{31}^{III} = \frac{2b\theta(1-A)}{1+l^2A^2}$ $(>0), m_{32}^{III} = -\frac{bd\theta^2A(1-A)}{g}$ $(<0), m_{21}^{III} = m_{23}^{III} = m_{33}^{III} = 0$ and $A = \sqrt{(\frac{g}{m_3\theta - gl^2})}$.

From Routh–Hurwitz criterion, E_3^{III} is locally asymptotically stable if and only if $A_1>0, A_3>0$ and $A_1A_2 - A_3 > 0$. See that $A_1A_2 - A_3 = m_{11}^{III}m_{13}^{III}m_{31}^{III} - m_{11}^{III}m_{22}^{III}(m_{11}^{III} + m_{22}^{III})$.

From the signs of those defined, $m_{ij}^{III}, i,j = 1,2,3$, it is easy to verify that A_3 will be positive if and only if $m_{22}^{III} < 0$. Also, A_1 will be positive when $(m_{11}^{III} + m_{22}^{III})$ is negative with $m_{22}^{III} < 0$. Then two cases may arise (1) either m_{11}^{III} is positive or (2) m_{11}^{III} is negative.

Case 1: If $m_{11}^{III} > 0$, then sign of $(m_{11}^{III}m_{13}^{III}m_{31}^{III})$ is negative and $\{m_{11}^{III}m_{22}^{III}(m_{11}^{III} + m_{22}^{III})\}$ is positive. Thus $(A_1A_2 - A_3)$ becomes negative, which violates R-H criterion of stability. So the system will be unstable when $m_{11}^{III} > 0$.

Case 2: If $m_{11}^{III} < 0$ then $(A_1A_2 - A_3)$ becomes positive. So the system is stable in this case. The sufficient conditions for m_{11}^{III} to be negative is $m_3 > \frac{2gl^2}{\theta}$. Also, m_{22}^{III} will be negative if $m_3 > (\frac{gl^2}{\theta} + \frac{g}{e^2\theta})$. It is to be noted that E_3^{III} exists when $m_3 > (\frac{gl^2}{\theta} + \frac{g}{\theta})$. Thus, E_3^{III} is stable when $m_3 > \max[(\frac{2gl^2}{\theta}), (\frac{gl^2}{\theta} + \frac{g}{e^2\theta}), (\frac{gl^2}{\theta} + \frac{g}{\theta})]$. Note that $\max[(\frac{2gl^2}{\theta}), (\frac{gl^2}{\theta} + \frac{g}{\theta})] = \frac{2gl^2}{\theta}$ as $l>1$. Therefore, E_3^{III} is stable when $m_3 > \max[(\frac{2gl^2}{\theta}), (\frac{gl^2}{\theta} + \frac{g}{e^2\theta})]$. Now, $\max[(\frac{2gl^2}{\theta}), (\frac{gl^2}{\theta} + \frac{g}{e^2\theta})]$ is $\frac{2gl^2}{\theta}$ or $(\frac{gl^2}{\theta} + \frac{g}{e^2\theta})$ according as $l > \frac{1}{e}$ or $l < \frac{1}{e}$. This proves the theorem.

7. Numerical simulation and discussion

From the existence conditions and stability analysis of the equilibria, the parameters e and $m_i, i = 1,2,3$ are recognized to be important. But, we cannot compare the dynamics of the model (2.3) in the e–m_i parameter plane as m_i are different for different i. So, we first rewrite all the conditions of different theorems in the original system parameters in Table 1 and compare the result in the α–λ parameter plane.

For all three functional responses, it is observed that the trivial equilibrium is always unstable saddle for all parametric values. When $\lambda < \frac{\mu}{K}$, E_1 is globally asymptotically stable if $\alpha < \frac{\delta}{K\theta}, \alpha < \frac{\delta(a+K)}{K\theta}$ and $\alpha < \frac{\delta(a^2+K^2)}{K^2\theta}$ for linear, Holling type II and III functional responses, respectively. Note that the net reproductive ratio, R_0, for all three cases, is given by $R_0 = \frac{\lambda S}{\mu}$. This R_0 gives the number of new cases acquired directly from a single infected prey. If $R_0<1$, the disease dies out, but if $R_0>1$, it remains endemic in the host population. Also observe that the net reproductive ratio increases in direct proportion to susceptible population, S. Thus, if the basic reproductive ratio be less than 1 even at maximum host level K (i.e. $\frac{\lambda K}{\mu} < 1$ or $\lambda < \frac{\mu}{K}$), the infection cannot spread in the host population. Biologically, it implies that if both the infection rate and the search rate of susceptible prey be low, the infected and predator population cannot survive and the system converges to the equilibrium where only healthy prey exists.

We present an example to confirm and visualize the observed results. We choose the fixed parameter values as described in Table 2 and vary only one ecological parameter α, predators' attack rate on susceptible prey, and one epidemiological parameter λ, the rate of infection. For the above set of parameter values we observe that E_1 will be stable if α be less than 0.005, 0.3, 0.25 for linear, type II and III, respectively, when $\lambda < 0.0053$. We select $\lambda = 0.003$ and the value of α as 0.004, 0.2 and 0.15 for linear, type II and III, respectively, and observe that all trajectories with different initial conditions [(30,10,15), (15,20,10), (10,5,5)] converge to the equilibrium where susceptible prey, S, exists in the form of a stable

Table 1
Comparison table for stability of the equilibria in original parameters

Functional resp. → equilibria ↓	Linear type	Holling type-II	Holling type-III
E_0	Always unstable	Always unstable	Always unstable
E_1	Globally stable if $\lambda<\frac{\mu}{K}$ $\alpha<\frac{\delta}{K\theta}$	Globally stable if $\lambda<\frac{\mu}{K}$ $\alpha<\frac{\delta(a+K)}{K\theta}$	Globally stable if $\lambda<\frac{\mu}{K}$ $\alpha<\frac{\delta(a^2+K^2)}{K^2\theta}$
E_2	Globally stable if $\lambda>\frac{\mu}{K}$ $\alpha<\frac{1}{\mu\theta}\left[\delta\lambda+\frac{r\beta\theta(\lambda K-\mu)}{r+\lambda K}\right]$ Globally stable if $\lambda<\frac{\mu}{K}$ $\alpha>\frac{\delta}{K\theta}$ Globally stable if	Globally stable if $\lambda>\frac{\mu}{K}$ $\alpha<\frac{a\lambda+\mu}{\lambda\mu\theta}\left[\delta\lambda+\frac{r\beta\theta(\lambda K-\mu)}{r+\lambda K}\right]$ Globally stable if $\lambda<\frac{\mu}{K}$ $\frac{\delta(K+a)}{K\theta}<\alpha<\frac{\delta(K+a)}{\theta(K-a)}$ Globally stable if	Globally stable if $\lambda>\frac{\mu}{K}$ $\alpha<\frac{a^2\lambda^2+\mu^2}{\lambda\mu^2\theta}\left[\delta\lambda+\frac{r\beta\theta(\lambda K-\mu)}{r+\lambda K}\right]$ Globally stable if $\lambda<\frac{\mu}{a}$ $\alpha>\frac{2\delta}{\theta}$ Globally stable if
E_3	$\lambda>\frac{\mu}{K}$ $\alpha>\frac{\delta\lambda}{\mu\theta}$ Limit cycle does not exist	$\frac{\mu}{K}<\lambda<\frac{2\mu}{K-a}$ $\frac{\delta(a\lambda+\mu)}{\mu\theta}<\alpha<\frac{\delta(K+a)}{\theta(K-a)}$ Limit cycle exists if $\alpha>\frac{\delta(a+K)}{\theta(K-a)}$ and $\lambda<\frac{2\mu}{K-a}$	$\lambda>\frac{\mu}{a}$ $\alpha>\frac{\delta}{\theta}+\frac{a^2\delta\lambda^2}{\theta\mu^2}$ Limit cycle does not exist
E^*	Always unstable	Always unstable	Always unstable

Table 2
Variables and parameters used in the models of susceptible prey-infected prey–predator population interaction

Variable/Parameters	Units	Definition	Default value
S	Number per unit designated area	Density of susceptible prey	–
I	Number per unit designated area	Density of infected prey	–
P	Number per unit designated area	Predator density	–
r	Per day	Growth rate of susceptible prey	3
K	Number per unit designated area	Carrying capacity	45
a	Number per unit designated area	Half-saturation constant	15
λ	Per day	Force of infection	–
α	Per day	Attack rate on susceptible prey	–
β	Per day	Attack rate on infected prey	0.05
μ	Per day	Death rate of infected prey Due to all causes except predation	0.24
θ	Per day	Conversion efficiency	0.4
δ	Per day	Natural death rate of predator	0.09

equilibrium (see Fig. 2). This indicates that the equilibrium E_1 is globally asymptotically stable for all three response functions. It is quite natural that in absence of predation and infection the equilibrium density of the susceptible population will approach to its carrying capacity (K) asymptotically.

Fig. 3 illustrates the parameter regions for the asymptotic stability of the axial equilibrium E_1 in $\lambda-\alpha$ parameter plane. Regions R_1, R_2, R_3 depict the stability areas of E_1 corresponding to linear, type II and III response functions. It is to be noted that the stability region increases gradually as we pass from linear mass-action response function to type II through type III. This indicates that the stability of the equilibrium E_1 is stronger for type II functional response compared to other two responses.

From Table 1 one can observe, if the infection rate be too high and the search rate of susceptible population be moderate then the predator population cannot survive and the system converges to the equilibrium where susceptible prey and infected prey coexist in the form of a stable

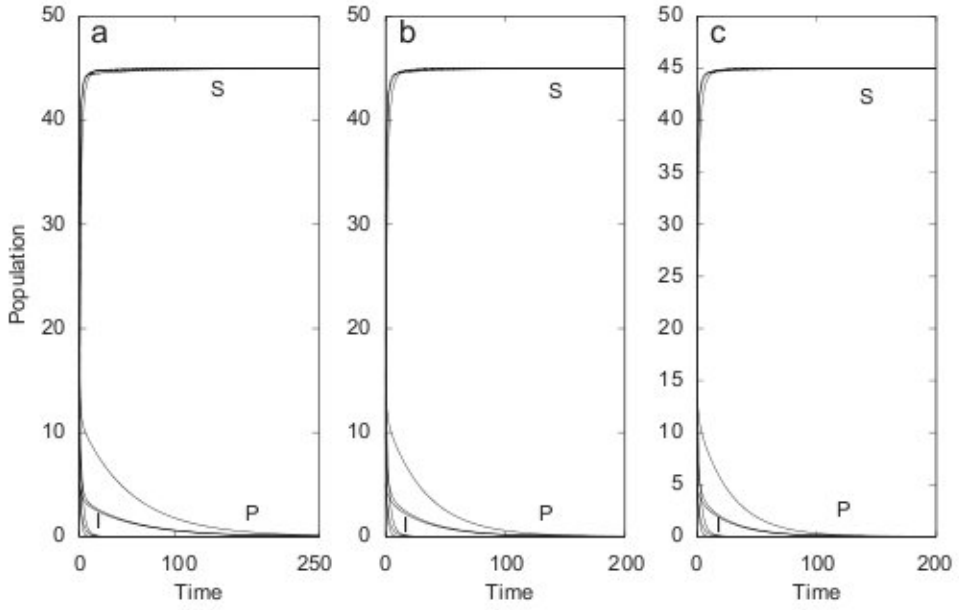

Fig. 2. Figures (a)–(c) depict the time series solutions of the model equations (4.1), (5.1) and (6.1) for S, I, and P, respectively, with initial values [30, 10, 15], [15, 20, 10] and [10, 5, 5] for the parameters as in Table 2. The values of α are, respectively, 0.004, 0.2 and 0.15 for linear, type II and III response functions and $\lambda = 0.003$ for all three response functions.

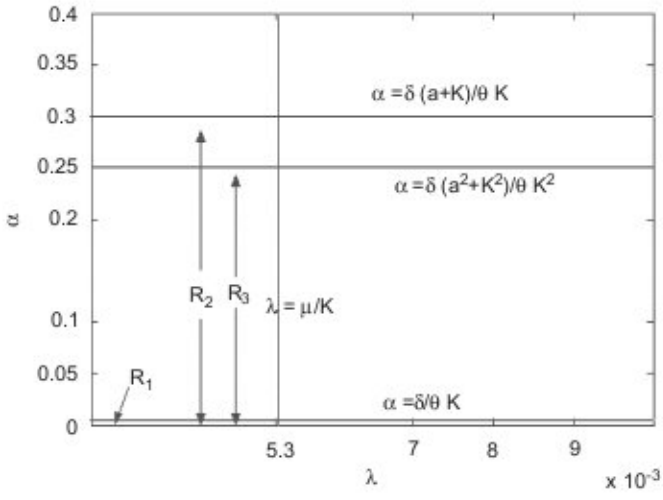

Fig. 3. Parameter regions for the global stability of the equilibrium E_1. In $R_1 = \{(\lambda,\alpha)/\lambda < \frac{\mu}{K}, \alpha < \frac{\delta}{K\theta}\}$, E_1^I attracts all positive solutions. In $R_2 = \{(\lambda,\alpha)/\lambda < \frac{\mu}{K}, \alpha < \frac{\delta(a+K)}{K\theta}\}$, E_1^{II} attracts all positive solutions. In $R_3 = \{(\lambda,\alpha)/\lambda < \frac{\mu}{K}, \alpha < \frac{\delta(a^2+K^2)}{K^2\theta}\}$, E_1^{III} attracts all positive solutions. Parameters are as in Table 2.

equilibrium. For the above set of parameter values (see Table 2) we observe that for the stability of E_2 the value of λ should be greater than 0.0053. Choosing $\lambda = 0.015$, we observe that α should be less than 0.0084, 2.71 and 2.63 for linear, Holling type II and III response functions, respectively. Thus, for $\lambda = 0.015$ and $\alpha = 0.005, 0.09, 0.05$ we observe that all trajectories converge to the predator-free equilibrium E_2 where susceptible prey and infected prey coexist in the form of a stable equilibrium (see Fig. 4). This indicates that the equilibrium E_2 is globally asymptotically stable for all three response functions.

From ecological point of view, when density of susceptible population becomes high, parasite can infect them quickly on a per capita basis because infection rate is high (i.e. $\lambda > \frac{\mu}{K}$). As a result, the parasite quickly spreads and S decreases when I increases. This result is also reflected in Fig. 4. Note that, the qualitative behavior of the solutions are same in all three response functions. In this case also, the parameter regions for the asymptotic stability of the predator-free equilibrium E_2 increases as we pass from linear response to type II through type III (see Fig. 5).

One can observe from Table 1 that the system can be stable around E_3 when infection rate is low or high and accordingly the predation rate must be low or high. For convenience we tabulate (see Table 3) the corresponding numerical ranges of λ and α for E_3 for the parameter values as in Table 1.

In case of lower infection rate, we observe that all trajectories with default values as in Table 3 converge to the disease-free equilibrium E_3 where susceptible prey and predator population coexist in the form of a stable equilibrium (see Fig. 6). Again observe that all trajectories with the default values in case of higher infection rate converge to the disease-free equilibrium E_3 where susceptible prey and predator population coexist in the form of a stable equilibrium (see Fig. 7). This indicates that the equilibrium E_3 is globally asymptotically stable for all three response functions with different infection and attack rates.

It is to be observed that in Holling type II and III species coexist in a stable form with enhanced predator population and depressed prey population levels, while in linear type I

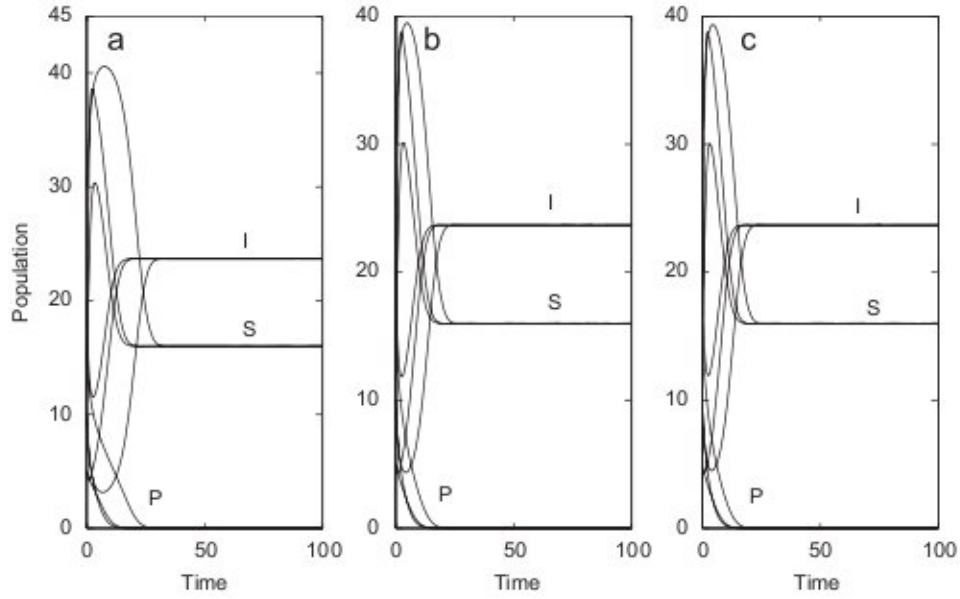

Fig. 4. Figures (a)–(c) depict the time series solutions of the model equations (4.1), (5.1) and (6.1), respectively, with initial values [30, 10, 15],[15, 20, 10] and [10, 5, 5]. The values of α are, respectively, 0.005, 0.09 and 0.05 for linear, type II and III response functions and $\lambda = 0.015$ for all three response functions.

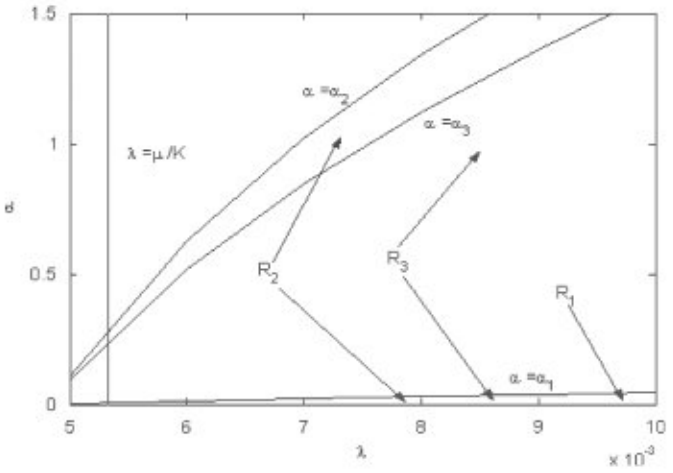

Fig. 5. Parameter regions for the global stability of the equilibrium E_2. In $R_1 = \{(\lambda, \alpha)/\lambda > \frac{\mu}{K}, \alpha < \frac{1}{\mu\theta}[\delta\lambda + \frac{r\beta\theta(\lambda K-\mu)}{r+\lambda K}] = \alpha_1\}$, E_2^I attracts all positive solutions. In $R_2 = \{(\lambda, \alpha)/\lambda > \frac{\mu}{K}, \alpha < \frac{\lambda a+\mu}{\lambda\mu\theta}[\delta\lambda + \frac{r\beta\theta(\lambda K-\mu)}{r+\lambda K}] = \alpha_2\}$, E_2^{II} attracts all positive solutions. In $R_3 = \{(\lambda, \alpha)/\lambda > \frac{\mu}{K}, \alpha < \frac{\lambda^2a^2+\mu^2}{\lambda\mu^2\theta}[\delta\lambda + \frac{r\beta\theta(\lambda K-\mu)}{r+\lambda K}] = \alpha_3\}$, E_2^{III} attracts all positive solutions. Parameters are as in Table 2.

predator and prey population both are depressed. In the last case prey population is maintained at densities less than 2% of its carrying capacity. This clearly violates the so-called "biological control paradox" which states that we cannot have both a low and stable prey equilibrium density (Luck, 1990). Also the general view regarding predators' increased search rate is to increase predator population is not inevitable in our model. Increased attack rate on susceptible prey can increase predator population level significantly in type II and III response functions but fails in case of linear mass-action response function (see Fig. 7). Another important observation is that at higher attack rate on susceptible prey, infection cannot persist permanently in the system, even when parasite successfully invade host population (i.e. R_0 may be greater than unity or $\lambda > \frac{\mu}{K}$). At this stage, if somehow, predators attack rate on healthy prey is decreased, the system will return to an equilibrium where susceptible and infected population coexist. This can be implemented by employing gamekeepers (Hudson et al., 1992a,b). Figs. 8a and b illustrate the parametric regions for the stability of the disease-free equilibrium, E_3, in α–λ parameter space for lower and higher infection rates, respectively. It is observed that in both the cases type III has larger stability regions compare to other two. This is not surprising because in a predator–prey interaction type III response behaves as if there were some prey refuges. This prey refuges reduce predation rates by decreasing encounter rates between predator and prey and thereby stabilize the predator–prey interaction for a wide range of parameter values (Anderson, 1984; Sih, 1987). Therefore, the stability of the equilibrium E_3 is much stronger in case of type III response function compared to the other two.

The most interesting dynamic behavior is observed in case of Holling type II functional response when the search rate exceeds some critical value. From the Table 1 we observe that when $\alpha > \frac{\delta(a+K)}{\theta(K-a)}$ with $\lambda < \frac{2\mu}{K-a}$, then system (5.1) possesses a stable limit cycles in the sp-plane. That is, when the attack rate on susceptible population, α, exceeds the critical value $\frac{\delta(a+K)}{\theta(K-a)}$ with $R_0 >$ or <1, system (5.1) exhibits a limit cycle in the sp-plane. Ecologically, when attack rate on susceptible prey is quite high, S decreases gradually and this causes I to decline and eventually be eradicated from the system. At low I or in absence of I, susceptible

Table 3
Parameter ranges and default values for lower and higher infection rate

Functional response	Range of λ	Default value of λ	Range of α	Default value of α
A. *Lower infection rate*				
Linear	$\lambda<0.0053$	0.003	$\alpha>0.005$	0.007
Type II	$\lambda<0.0053$	0.003	$0.3<\alpha<0.45$	0.35
Type III	$\lambda<0.0160$	0.003	$\alpha>0.45$	0.50
B. *Higher infection rate*				
Linear	$\lambda>0.0053$	0.008	$\alpha>0.0075$	0.3
Type II	$\lambda>0.0053$	0.008	$0.3375<\alpha<0.45$	0.4
Type III	$\lambda>0.0160$	0.017	$\alpha>0.5098$	0.8

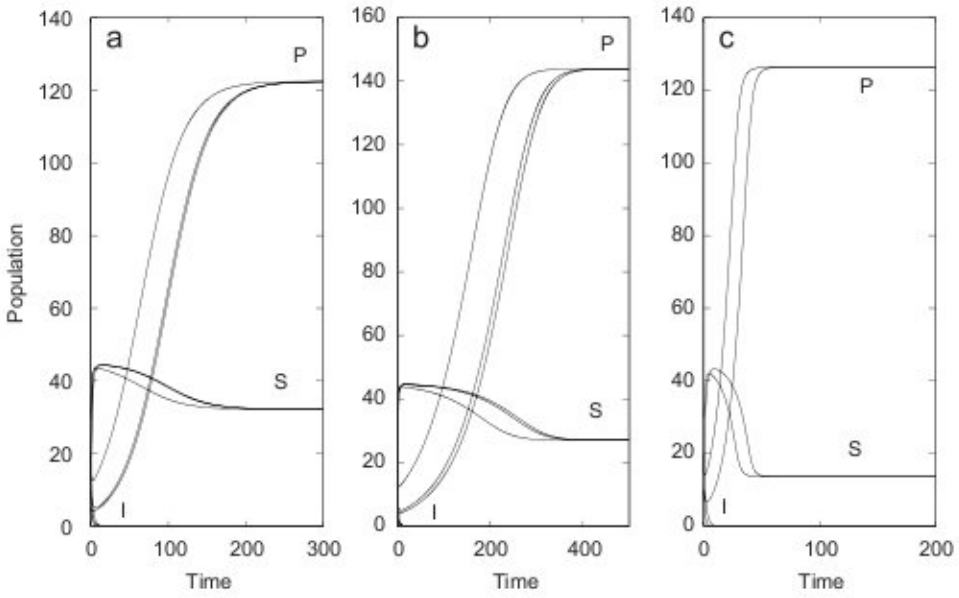

Fig. 6. Figures (a)–(c) depict the time series solutions of the model equations (4.1), (5.1) and (6.1), respectively, with initial values [30, 10, 15], [15, 20, 10] and [10, 5, 5]. The values of α are, respectively, 0.007, 0.35 and 0.5 for linear, type II and III response functions and $\lambda = 0.003$ for all three response functions.

population S increases rapidly as much of their resources remains unused. At that time, the increased attack rate on susceptible prey causes predator population also to increase. Once abundant, predator cannot completely control susceptible hosts because predators become satiated and begins to oscillate. Fig. 9 depicts a limit cycle oscillations of system (5.1) when $\alpha = 0.5$ (which is greater than the critical value 0.45) and $\lambda = 0.008$ with same initial values. We do not observe limit cycle oscillations in other two functional responses. Thus, in a host–parasite system with a type II functional response and very high attack rate on healthy prey produces complex but biologically relevant behavior in the host–parasite system.

For all three functional responses it is observed that the interior equilibrium, where all three species exist, is unstable for all parametric values. The interior equilibrium becomes a hyperbolic saddle with stable manifold of dimension two. This stable manifold separates the domains of attraction of the SI and SP equilibrium points. Thus, if the initial value of the system is contained in the invariant domain which contains the equilibrium point E_2, the solution will eventually approach E_2 under suitable parametric conditions and if the initial value of the system is contained in the invariant domain which contains the equilibrium point E_3, the solution will eventually approach E_3 under suitable parametric conditions.

Observe that the solution of (5.1) with initial value (30,10,15) approaches a limit cycle surrounding E_3^{II} in the SP-plane indicating that the initial state is in the domain of attraction of SP-plane (see Figs. 10a and b), while the solution of (5.1) with initial value (10,5,5) approaches the equilibrium E_2^{II} indicating that the initial state is in the domain of attraction of SI-plane (see Figs. 10(c) and (d)). Similar situation is also observed for Holling type III response function.

Ecologically, instability of the interior equilibrium is attributed to the harmful effect of the infected prey on the predator. The predator population cannot coexist with the infected population (note that the derivative of the r.h.s. of the second equation of system (2.3) w.r.t. P is always negative for all three response functions) and this event forces the interior equilibrium to be unstable for all parametric values.

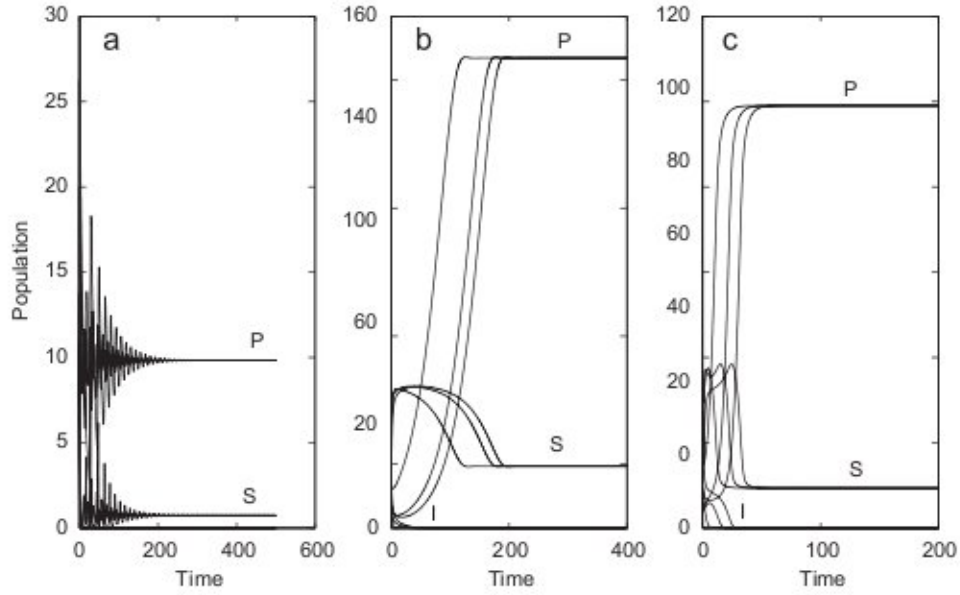

Fig. 7. Figures (a)–(c) depict the time series solutions of the model equations (4.1), (5.1) and (6.1), respectively, with initial values [30, 10, 15], [15, 20, 10] and [10, 5, 5]. The values of α are, respectively, 0.3, 0.4 and 0.8 for linear, type II and III response functions and $\lambda = 0.008$ for linear and type II and $\lambda = 0.017$ for type III.

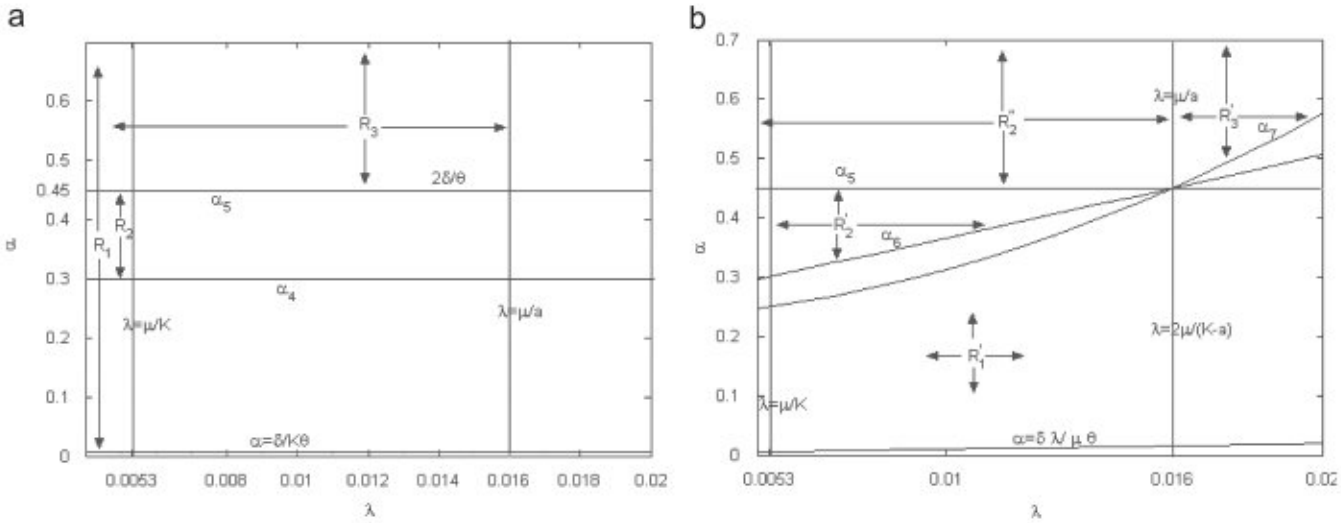

Fig. 8. (a) Parameter regions for the global stability of the equilibrium E_3 for lower infection rate. In $R_1 = \{(\lambda, \alpha)/\lambda < \frac{\mu}{K}, \alpha > \frac{\delta}{K\theta}\}$, E_3^I attracts all positive solutions. In $R_2 = \{(\lambda, \alpha)/\lambda < \frac{\mu}{K}, \alpha_4 = \frac{\delta(K+a)}{K\theta} < \alpha < \frac{\delta(K+a)}{\theta(K-a)} = \alpha_5\}$, E_3^{II} attracts all positive solutions. In $R_3 = \{(\lambda, \alpha)/\lambda < \frac{\mu}{a}, \alpha > \frac{2\delta}{\theta}\}$, E_3^{III} attracts all positive solutions. Parameters are as in Table 2. (b) Parameter regions for the global stability of the equilibrium E_3 for higher infection rate. In $R_1' = \{(\lambda, \alpha)/\lambda > \frac{\mu}{K}, \alpha > \frac{\lambda\delta}{\mu\theta}\}$, E_3^I attracts all positive solutions. In $R_2' = \{(\lambda, \alpha)/\frac{\mu}{K} < \lambda < \frac{2\mu}{K-a}, \alpha_6 = \frac{\delta(\mu+\lambda a)}{\mu\theta} < \alpha < \frac{\delta(K+a)}{\theta(K-a)} = \alpha_5\}$, E_3^{II} attracts all positive solutions. In $R_2'' = \{(\lambda, \alpha)/\lambda < \frac{2\mu}{K-a}, \alpha > \frac{\delta(K+a)}{\theta(K-a)} = \alpha_5\}$, limit cycles exist around E_3^{II}. In $R_3' = \{(\lambda, \alpha)/\lambda > \frac{\mu}{a}, \alpha > \frac{\delta}{\theta} + \frac{\delta a^2 \lambda^2}{\theta\mu^2} = \alpha_7\}$, E_3^{III} attracts all positive solutions. Parameters are as in Table 2.

Our model gives several insights into switches between oscillating and stable equilibria. It is observed that infection may destabilize otherwise stable healthy predator–prey interaction, while predator may destabilize a stable host–parasite system which is otherwise stable. The specific behavior of the eco-epidemiological system depends crucially on the infection rate and the attack rate of the predator on susceptible prey. Our overall mathematical and biological studies reveal that in host–parasite–predator system, where prey is infected by a lethal disease, coexistence of all the three species is never possible (contrary to Venturino, 1995; Chattopadhyay and Arino, 1999; Xiao and Chen, 2001), instead only healthy or disease-free or predator-free or even a fluctuating disease-free system can be obtained by regulating the two key parameters. It is also observed that the biological control paradox is not intrinsic to an eco-epidemiological model. Our model also has wide applicability in a variety of

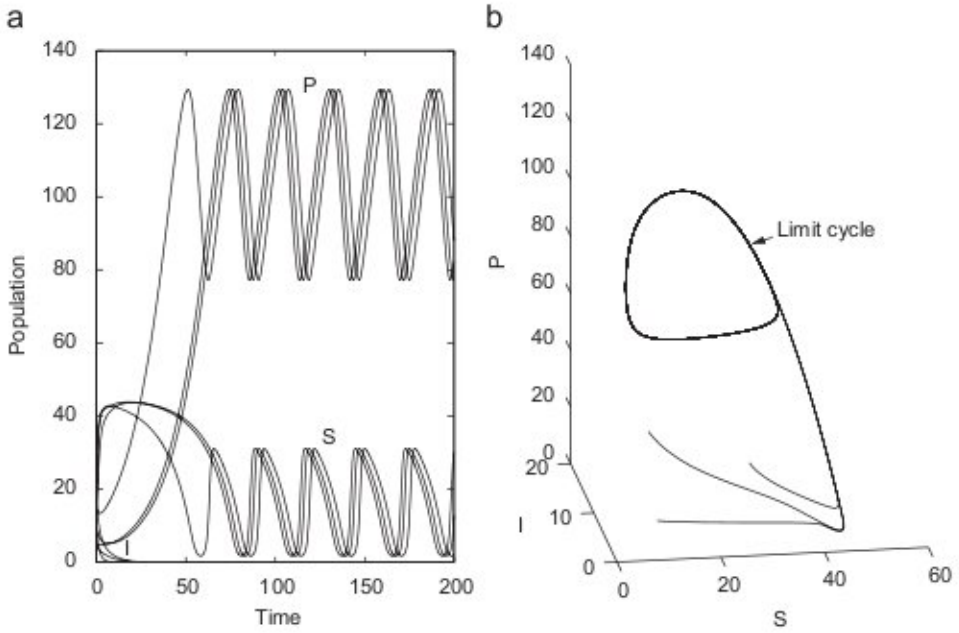

Fig. 9. Figures (a) and (b) depict, respectively, the time series solution and the trajectory of the model equation (5.1) (i.e. Holling type II) with initial values [30, 10, 15], [15, 20, 10] and [10, 5, 5]. Here $\lambda = 0.008$ and $\alpha = 0.5$ (which is greater than the critical value 0.45).

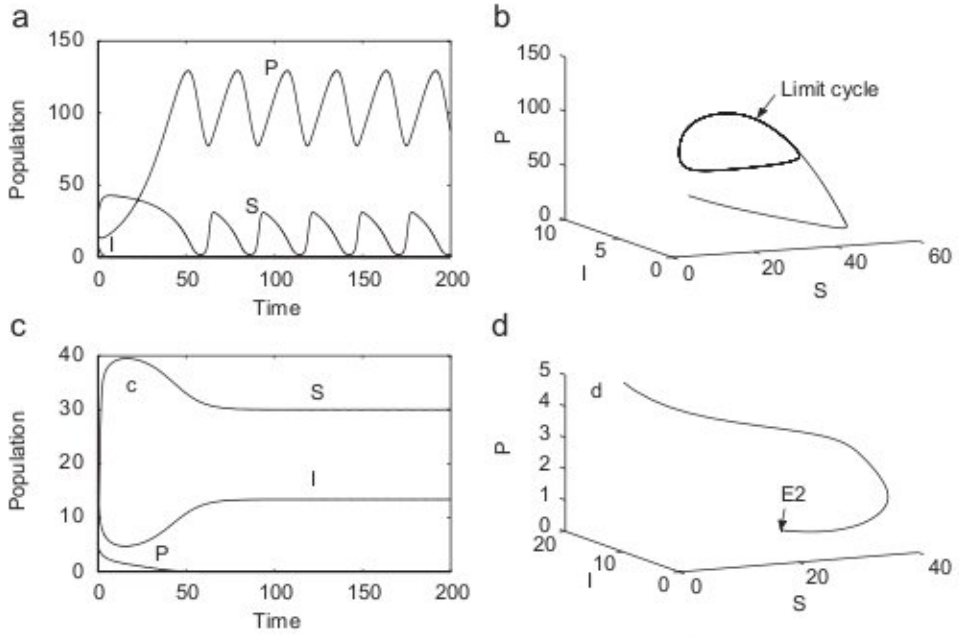

Fig. 10. Solution of (5.1) with initial values [30,10,15] (Figs. 10(a) and (b)) and [5,15,5] (Fig. 10(c) and (d)) for $\lambda = 0.008$ and $\alpha = 0.5$.

host–parasite–predator systems as it incorporates different response functions. It is now worthwhile to study an eco-epidemiological situations of upland estates in England and Scotland.

A case study: The population biology of red grouse and its predator for 10 years has been considered as a case study. For this study the most of the parameter values have been taken from the published papers and others have been estimated. The per capita birth rate and the natural death rate of grouse are 0.15 and 0.0875 per month, respectively (Dobson and Hudson, 1992). Thus, the per capita intrinsic growth rate of grouse is 0.0630 per month. Maximum number of grouse observed per square kilometer is around 100 (Dobson and Hudson, 1992; Hudson et al., 1992b). The value of carrying capacity is assumed to be 25% higher than the maximum observed value, therefore the value of K is assumed to be 125 grouse per square kilometer. An adult fox takes on average one or two infected grouse a week

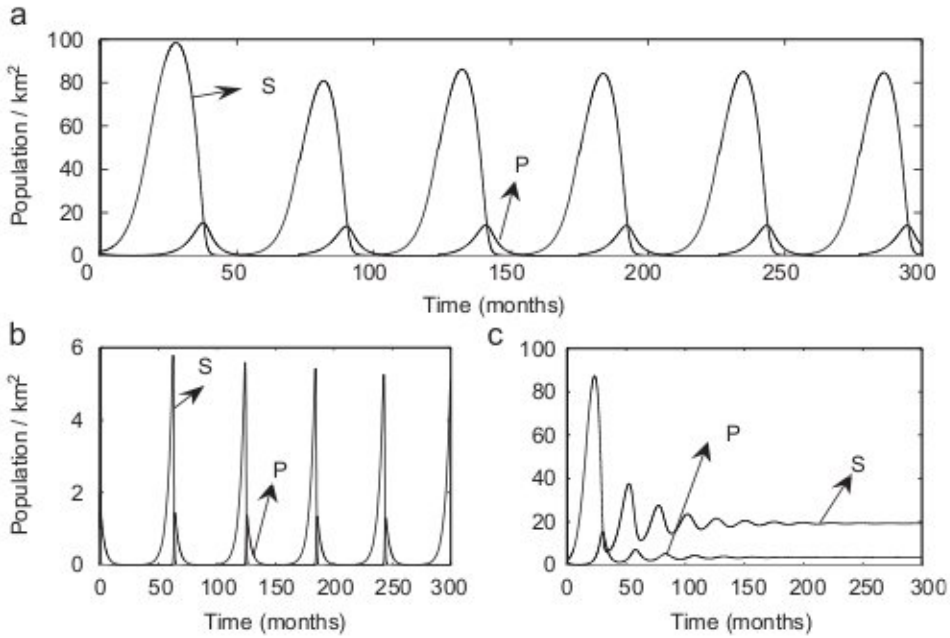

Fig. 11. Changes in numbers of grouse and fox per square kilometer: (a) typical cycles with a time period of 4–5 years for type II response function, (b) damped oscillation with low population densities for type I response function and (c) stable population densities for type III response function.

(Hudson et al., 1992a), therefore 4–8 grouse per month. Thus, we select $\beta = 6$ per predator per month. The value of α is assumed to be 10 times smaller than β, so that $\alpha = 0.6$ per predator per month. Instantaneous death rate of infected grouse due to all causes except the predation is 0.087525 per month (Jenkins et al., 1964), therefore, we select $\mu = 0.0876$. The range of infection rate is 1.6×10^{-1} to 0.6 per host per year (Dobson and Hudson, 1992), so we assume $\lambda = 0.0317$ per host per month. The instantaneous death rate of predator (δ) is assumed as 0.075 per month and the values of a and θ are taken as 20 grouse per square kilometer and 0.26 per month. Assuming that the infection has no lethal effect on the predator, then the qualitative behavior of system (2.3) corresponds closely to the field data of grouse population observed by Hudson et al. (1992a,b) and Potts et al. (1984).

It is observed that the grouse population oscillates when functional response is of type II and the period of oscillation is 4–5 years (Fig. 11(a)). But, for linear type response function, the system exhibits damped oscillation with very low prey density, whereas for type III response function the system becomes stable (see Figs. 11(b) and (c)). The above observations clearly demonstrate that habitat structure may be one of the reasons of regular fluctuation in population density in addition to density-dependent regulatory factors viz. competition, predation, parasitism and dispersal (May, 1981) and alter the predator–prey dynamics significantly. We like to mention here that Hudson and Dobson (1990) concluded with experimental observations that in some estates the grouse population cannot exhibit regular fluctuation, rather shows stable behavior. Thus our simulation results are in accordance with the field and experimental findings.

Acknowledgments

We thank two anonymous reviewers for their valuable comments and helpful suggestions.

References

Alstad, D., 2001. Basic Populas Models of Ecology. Prentice-Hall, Englewood Cliffs, NJ.

Anderson, O., 1984. Optimal foraging by largemouth bass in structured environments. Ecology 65, 851–861.

Anderson, T.W., 2001. Predator responses, prey refuges and density-dependent mortality of a marine fish. Ecology 82 (1), 245–257.

Beltrami, E., Carroll, T.O., 1994. Modelling the role of viral disease in recurrent phytoplankton blooms. J. Math. Biol. 32, 857–863.

Beretta, E., Kuang, Y., 1998. Modelling and analysis of a marine bacteriophage infection. Math. Biosci. 149, 57–76.

Birkhoff, G., Rota, G., 1989. Ordinary Differential Equations, fourth ed. Wiley, Canada.

Chattopadhyay, J., Arino, O., 1999. A predator–prey model with disease in the prey. Nonlinear Anal. 36, 747–766.

Chattopadhyay, J., Bairagi, N., 2001. Pelicans at risk in Salton Sea—an eco-epidemiological study. Ecol. Modelling 136, 103–112.

Chattopadhyay, J., Pal, S., 2002. Viral infection on phytoplankton zooplankton system—a mathematical model. Ecol. Modelling 151, 15–28.

Chattopadhyay, J., Srinivasu, P.D.N., Bairagi, N., 2003. Pelicans at risk in Salton Sea—an eco-epidemiological model—II. Ecol. Modelling 167, 199–211.

Dobson, A.P., Hudson, P.J., 1992. Regulation and stability of a free-leaving host–parasite system. *Trichostrongylus tenuis* in red grouse. II. Population models. J. Anim. Ecol. 61, 487–500.

Dwyer, G., Dushoff, J., Yee, S.H., 2004. Generalist predators, specialist pathogens and insect outbreaks. Nature 43, 341–345.

Freedman, H.I., 1990. A model of predator–prey dynamics as modified by the action of parasite. Math. Biosci. 99, 143–155.

Gonzalez, M.R., Hart, C.M., Verfaillie, J.R., Hurlbert, S.H., 1998. Salinity and fish effects on Salton Sea microecosystems: water chemistry and nutrient cycling. Hydrobiologia 381, 105–128.

Hadeler, K.P., Freedman, H.I., 1989. Predator–prey population with parasite infection. J. Math. Biol. 27, 609–631.

Hall, S.R., Duffy, M.A., Caceres, C.E., 2005. Selective predation and productivity jointly drive complex behavior in host–parasite systems. Am. Nat. 165 (1), 70–81.

Hethcote, H.W., Wang, W., Han, L., Ma, Z., 2004. A predator–prey model with infected prey. Theor. Popul. Biol. 66, 259–268.

Holling, C.S., 1959. Some characteristics of simple types of predation and parasitism. Can. Entomologist 91, 385–398.

Hudson, P.J., Dobson, A.P., 1990. Red grouse population cycles and the population dynamics of the caecal nematode *Trichostrongylus tenuis*. In: Lance, A.N., Lawton, J.H. (Eds.), Red Grouse Population Processes. British Ecological Society and Royal Society for the Protection of Birds, pp. 2256–2258.

Hudson, P.J., Dobson, A.P., Newborn, D., 1992a. Do parasites make pray vulnerable to predation? Red grouse and parasites. J. Anim. Ecol. 61, 681–692.

Hudson, P.J., Newborn, D., Dobson, A.P., 1992b. Regulation and stability of a free-leaving host–parasite system, *Trichostrongylus tenuis* in red grouse. I. Monitoring and parasite reduction experiment. J. Anim. Ecol. 61, 477–486.

Hudson, P.J., Dobson, A.P., Newborn, D., 1998. Prevention of population cycles by parasite removal. Science 282, 2256–2258.

Ives, A.R., Murray, D.L., 1997. Can sublethal parasitism destabilize predator–prey population dynamics? A model of snowshoe hares predators, and parasites. J. Anim. Ecol. 66, 265–278.

Jenkins, D., Watson, A., Miller, G.R., 1964. Predation and red grouse populations. J. Appl. Ecol. 1, 183–195.

Korpimaki, E., Norrdahl, K., 1991. Numerical and functional responses of kestrels, short-eared owls, and long-eared owls to vole densities. Ecology 72, 814–826.

Lakshmikantham, V., Leela, S., 1969. Differential and Integral Inequalities, vol. 1. Academic Press, New York.

Luck, R.F., 1990. Evaluation of natural enemies for biological control: a behavior approach. Trends Ecol. Evolution 5, 196–199.

May, R.M., 1981. Theoretical Ecology. Blackwell Scientific Publications, Oxford.

Moore, J., 2002. Parasites and the Behaviour of Animals. Oxford University Press, Oxford.

Murray, D.L., Carry, J.R., Keith, L.B., 1997. Interactive effects of sublethal nematodes and nutritional status on snowshoe hare vulnerability to predation? J. Anim. Ecol. 66, 250–264.

Packer, C., Holt, R.D., Hudson, P.J., Lafferty, K.D., Dobson, A.P., 2003. Keeping the herds healthy and alert: implications of predator control for infectious disease. Ecol. Lett. 6, 792–802.

Potts, G.R., Tapper, S.C., Hudson, P.J., 1984. Population fluctuations in red grouse: analysis of bag records and a simulation model. J. Anim. Ecol. 53, 21–36.

Ricklefs, R.E., Miller, G.L., 2000. Ecology, fourth ed. Williams and Wilkins Co., Inc.

Sih, A., 1987. Prey refuges and predator–prey stability. Theor. Popul. Biol. 31, 1–12.

Sih, A., Crowley, P., McPeek, M., Petranka, J., Strohmeier, K., 1985. Predation, competition, and prey communities: a review of field experiments. Annu. Rev. Ecol. Syst. 16, 269–311.

Venturino, E., 1995. Epidemics in predator–prey models: disease in the prey. In: Arino, O., Axelrod, D., Kimmel, M., Langlais, M. (Eds.), Mathematical Population Dynamics: Analysis of Heterogeneity, vol. 1. pp. 381–393.

Venturino, E., 2002. Epidemics in predator–prey models: disease in the predators. IMA J. Math. Appl. Med. Biol. 19, 185–205.

Xiao, Y., Chen, L., 2001. Modelling and analysis of a predator–prey model with disease in the prey. Math. Biosci. 171, 59–82.